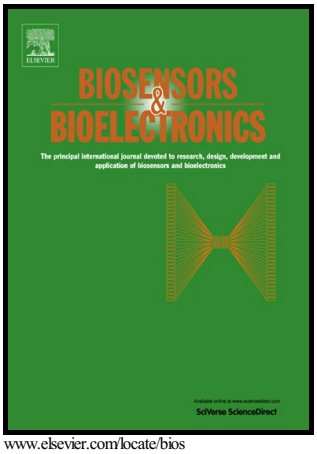

www.elsevier.com/locate/bios

MMP2-sensing Up-conversion Nanoparticle for Fluorescence Biosensing in Head and Neck Cancer Cells

Yung-Chieh Chan, Chieh-Wei Chen, Ming-Hsien Chan, Yu-Chan Chang, Wei-Min Chang, Li-Hsing Chi, Hui-Ming Yu, Yuan-Feng Lin, Din Ping Tsai, Ru-Shi Liu, Michael Hsiao

PII: S0956-5663(16)30049-5
DOI: http://dx.doi.org/10.1016/j.bios.2016.01.049
Reference: BIOS8389

To appear in: *Biosensors and Bioelectronic*

Received date: 19 November 2015
Revised date: 8 January 2016
Accepted date: 18 January 2016

Cite this article as: Yung-Chieh Chan, Chieh-Wei Chen, Ming-Hsien Chan, Yu-Chan Chang, Wei-Min Chang, Li-Hsing Chi, Hui-Ming Yu, Yuan-Feng Lin, Din Ping Tsai, Ru-Shi Liu and Michael Hsiao, MMP2-sensing Up-conversion Nanoparticle for Fluorescence Biosensing in Head and Neck Cancer Cells *Biosensors and Bioelectronic,* http://dx.doi.org/10.1016/j.bios.2016.01.049

MMP2-sensing Up-conversion Nanoparticle for Fluorescence Biosensing in Head and Neck Cancer Cells

Yung-Chieh Chan[1], Chieh-Wei Chen[2], Ming-Hsien Chan[2], Yu-Chan Chang[1], Wei-Min Chang[1], Li-Hsing Chi[1,3], Hui-Ming Yu[1], Yuan-Feng Lin[4], Din Ping Tsai[5,6*], Ru-Shi Liu[1,2,5,7*], and Michael Hsiao[1*]

[1] Genomics Research Center, Academia Sinica, Taipei, Taiwan,

[2] Department of Chemistry, National Taiwan University, Taipei 106, Taiwan,

[3] Division of Oral and Maxillofacial Surgery, Department of Dentistry, Taipei Medical University Hospital, Taipei, Taiwan.

[4] Graduate Institute of Clinical Medicine, College of Medicine, Taipei Medical University, Taipei, Taiwan,

[5] Research Center for Applied Science, Academia Sinica, Taipei 115, Taiwan,

[6] Department of Physics, National Taiwan University, Taipei 116, Taiwan

[7] Department of Mechanical Engineering and Graduate Institute of Manufacturing Technology, National Taipei University of Technology, Taipei 106, Taiwan

Correspondence to: Dr. Michael Hsiao, E-mail: mhsiao@gate.sinica.edu.tw, Dr. Ru-Shi Liu, E-mail: rsliu@ntu.edu.tw, or to: Dr. Din Ping Tsai, E-mail: dptsai@phys.ntu.edu.tw

Abstract

Upconversion nanoparticles (UCNPs) have extensive biological-applications because of their bio-compatibility, tunable optical properties and their ability to be excited by infrared radiation. Matrix metalloproteinases (MMPs) play important roles in extracellular matrix remodelling; they are usually found to significantly increase during cancer progression, and these increases may lead to poor patient survival. In this study, we produced a biosensor that can be recognized by MMP2 and then be unraveled by the attached quencher to emit visible light. We used 3.5-nm gold nanoparticles as a quencher that absorbed emission from UCNPs at a wavelength of 540 nm. The biosensor consists of an upconversion nanoparticle, MMP2-recognized polypeptides and quenchers. Here, UCNPs consisting of $NaYF_4$:Yb^{3+}/Er^{3+} were prepared via a high temperature co-precipitation method while protecting the oleic acid ligand. To improve the biocompatibility and modify the UCNPs with a polypeptide, they were coated with a silica shell and further conjugated with MMP-recognizing polypeptides. The polypeptide has two ends of featuring carboxylic and thiol groups that react with UCNPs and AuNPs, and the resulting nanoparticles were referred to as UCNP@p-Au. According to the *in vitro* cell viability analysis, UCNP@p-Au exhibited little toxicity and biocompatibility in head and neck cancer cells. Cellular uptake studies showed that the MMP-based biosensor was activated by 980-nm irradiation to emit green light. This MMP-based biosensor may serve as sensitive and specific molecular fluorescent probe in biological-applications.

1. Introduction

Extracellular matrix remodelling is an important process during cancer progression(Holle et al. 2015). Most malignant tumour cells destroy matrix barriers to allow cancer cells to invade connective tissue and metastasize to distant organs (Gong et al. 2014; Theocharis et al. 2015). A zinc-dependent matrix metalloproteinase (MMP) is usually involved in extracellular matrix remodelling due to the unique proteolytic ability of this family (Eftekhary et al. 2015; Yang et al. 2015). MMP overexpression has been identified as a hallmark of cancer progression, which involves metastasis and angiogenesis (Banerjee and Resat 2015; Zou et al. 2015). MMP2 and MMP9 are gelatinases, which can degrade type IV extracellular protein and nonfibrillar collagens (Kwan et al. 2004). MMP2 expression is significantly increased in many types of cancers, including breast cancer, and head and neck cancer(Adabi et al. 2015; Jafarian et al. 2015; Zhang et al. 2015). MMP2 has attracted increasing attention in the field of diagnosis and targeted therapy (Liu et al. 2015a; Xu et al. 2015). A surface-enhanced Raman spectroscopy-based platform was developed to sense MMP2 using an MMP2-recognized peptide (Gong et al. 2015). Recently, the MMP2- and caspase-3-specific peptides were integrated in a dual FRET-based fluorescent probe(Li et al. 2015). Folic acid is a well-known moiety targeted by for anticancer drugs because of the high affinity of folate receptors(Frankowski et al. 2012). Upconversion fluorescence generates a multi-emission spectrum, and consists of the conversion of long-wavelength absorption to short-wavelength emission, permitting near IR radiation to produce visible light. Rare earth elements are usually used to synthesize upconversion nanomaterials (Shao et al. 2015; Zhong et al. 2015). Upconversion nanoparticle (UCNP) consists of a sensitizer and an activator doping host nanomaterial(Chen et al. 2015). Yb^{3+}-Er^{3+} is usually used as a sensitizer and an activator in upconversion nanoparticles.

In this study, we fabricated an MMP2-sensing upconversion nanoparticle conjugated to AuNPs, named UCNP@p-Au. These UCNP@p-Au particles consist of $NaYF_4$:Yb^{3+}/Er^{3+} decorated with an MMP2-recognizing peptide and folic acid, and are conjugated to a gold nanoparticle. Our results showed these novel MMP2-sensing AuNPs can be endocytosed by head and neck cancer cells and are biocompatible with little cellular toxicity. Upon infrared irradiation, these NPs can induce cells to emit green light. This NIR-induced MMP2 sensor can be used in animal models and clinical trials.

2. Materials and Methods

2.1. Materials

All chemicals were obtained from commercial suppliers. $Yb(CH_3CO_2)_3•4H_2O$ (99.9%), $Er(CH_3CO_2)_3•xH_2O$ (99.9%), $Y(CH_3CO_2)_3•xH_2O$ (99.9%), NH_4F (98+%), 1-octadecene (90%), Oleic acid (OA; 90%), (3-Aminopropyl)triethoxysilane (APTES; 98%), N-(3-dimethylaminopropyl)-N-ethylcarbodiimide hydrochloride (EDC), cyclohexane, N-hydroxysuccinimide (NHS), and folic acid were purchased from Sigma-Aldrich (Missouri, USA). 4',6-diamidino-2-phenylindole (DAPI) and Alexa Fluor 647 were purchased from Invitrogen.

2.2. Synthesis of upconversion nanoparticle

Upconversion nanoparticles were constructed from $NaYF_4:Yb^{3+}/Er^{3+}$ and synthesized using a high-temperature co-precipitation method as previously described (Chen et al. 2015). $Y(CH_3CO_2)_3•xH_2O$ (0.4 mmol), $Yb(CH_3CO_2)_3•4H_2O$ (0.1 mmol) and $Er(CH_3CO_2)_3•xH_2O$ (0.1 mmol) were dissolved in OA and 1-octadecene (3:7; 12.5 ml) at 150 °C under nitrogen for 30 min (Sigma, USA). The dissolved lanthanide salts were then cooled down to 50 °C and stirred with methanol solution containing NH_4F (2 mmol) and NaOH (1.25 mmol) for 30 min. The methanol was removed by heating the solution to 100 °C for 30 min. Subsequently, the solution was heated to 290 °C for 2 hours and cooled to room temperature. The $NaYF_4:Yb^{3+}/Er^{3+}$ nanoparticles were precipitated with absolute ethanol and recovered by centrifugation at 6000 rpm for 10 min. The prepared nanoparticles were stored in cyclohexane.

2.3.Conjugation of UCNP@peptide and Gold nanoparticle

The UCNPs were coated with silica shells and modified with amino groups using a reverse micro-emulsion method (Li et al. 2011). UCNP was added to a 12 ml mixture of cyclohexane and Polyoxyethylene (5) nonylphenylether (branched; IGEPAL CO-520) for 1 hour under constant stirring. Subsequently, 0.1 ml of ammonium solution

was then added, and the mixture was incubated for an additional hour. A 3-nm-thick of the silica shell was constructed at 3 nm by slowly adding 20 μl of Tetraethyl orthosilicate (TEOS). The amino groups were grafted onto the UCNP@ SiO_2 by slowly adding 0.1 ml of APTES. The UCNP@SiO_2 was collected and washed using methanol precipitation and centrifuging at 8000 rpm for 20 min. MMP2-recognizing peptides were synthesized at the Peptide Synthesis Core Facility (Genomics Research Center, Academia Sinica, Taiwan). The N-terminus was acetylated and included cysteine. The amino acid sequence is CSGAVRWLLTA. The MMP2-recognizing sequence is referred to as "SGAVRWLLTA" (Chen et al. 2002). The C-terminus of the peptide was conjugated to UCNP@SiO_2-NH_2 by NHS/EDC coupling method. The peptide, folic acid, NHS and EDC were mixed at a molar ratio of 2:1:4:2 in DDW at room temperature for 1 hour. Subsequently, the activated peptide intermediates were modified using 10 mg of UCNP@SiO_2-NH_2 for 12 hours with gently stirring. The 3.5 nm gold nanoparticle was synthesized using $NaBH_4$ (reduction agent) and citric acid (capping ligand). Solutions containing different concentrations of gold nanoparticle were added to the UCNP@peptide (UCNP@p) at 4 ℃ for 12 hours. The UCNP@p-Au particles were purified by centrifuging at 10000 rpm for 5 min.

2.4. Cell culture and cell viability

Human head and neck cancer cell lines, including Cal27, HSC3, HSC4, CA922, SAS, YD15 and TW2.6, were grown in D-MEM medium (Invitrogen, USA). FADU cells were grown in MEM medium (Invitrogen, USA). OEC-M1 cells were grown in RPMI medium (Invitrogen, USA). All cell culture media were supplemented with 10% FBS (Invitrogen, USA) and 1% of Penicillin-Streptomycin-Glutamine cocktail (GIBCO, USA). All cells were incubated at 37℃in a CO_2 incubator containing 5% CO_2. A 96-well plate was inoculated with 2000 cells per well and incubated for 12 hours. The plate was then incubated with serial dilution of UCNP@p-Au (250, 83, 27, 9, 3 and 1μg/ml). After 48 hours of incubation, an Alamar blue assay was performed according to the manufacturer's protocol. The Alamar blue assay was conducted on a SpectraMax M2 instrument using excitation/emission wavelengths of 560/590 nm (Molecular Devices, California, USA). The data from six independent tests are presented as the means± SDs.

2.5. Western blot analysis

A western blot analysis was performed as previously reported(Liu et al. 2015b). The protein concentration was measured with a Pierce BCA assay (Thermo, USA). The primary antibody against MMP-2 was diluted in 5% BSA/PBST buffer (1:1000, cell signalling, MA, USA). The folate receptor 2 (FOLR2) antibody was diluted in 5% BSA/PBST buffer (1:1000, cell signalling, MA, USA). Anti–β-actin was used as internal control (1:5,000, Sigma-Aldrich, MO, USA).

2.6. MMP2 overexpression construct and stable cell line

The cDNA expression vector (pLAS3W.Ppuro), lentiviral envelope and packing plasmids (pMDG and pCMV-Δ8.91) were purchased from the National RNAicore facility (Academia Sinica, Taiwan). The MMP2 cDNA construct was purchased from Clontech (USA). MMP2 cDNA was subcloned into pLAS3W.Ppuro. The lentiviral expression constructs and blank vector were co-transfected into 293T cells with both of pMDG and pCMV-Δ8.91 plasmids, respectively, using the calcium phosphate transfection method, followed by lentivirus production and selection with puromycin (2 μg/ml) for one week. The MMP2-containing lentiviruses were collected and used to infect cells in the present of polybrene (2 μg/ml). The conditioned media were collected from an overnight culture in serum-free medium from Cal27/VC and Cal27/MMP2.

2.7. Cell sensing imaging analysis

A 12-well plate containing cover slips was inoculated with 5000 cells per well and incubated for 12 hours. Subsequently, 10 μg/ml of UCNP@p-Au was added and the plated was cultured for 12 hours. The cells were then fixed with 4% paraformaldehyde and stained with anti-alpha-tubulin (1:300 in 5% BSA/PBS). The stained slides were mounted using a DAPI-containing mounting gel. The images were captured with a Nikon Ti-E inverted microscope at an excitation wavelength of 980 nm from a laser source (Nikon, Taiwan). The secondary antibody against anti-alpha-tubulin was conjugated with Alexa 647 (Invitrogen, USA)

2.8. Identification of upconversion nanoparticle

The morphology of the UCNP, UCNP@p and UCNP@p-Au particles was determined using a JEM-2100F transmission electron microscope with an electron gun operating at 100 keV. The emission spectra of UCNP and its derivatives were characterized based on a photoluminescence spectrum at an excitation of 980 nm using SpectraMax M2 (Molecular Devices, California, USA).

3. Results and discussion

3.1. Design and fabrication of MMP2-recognized UCNP@p-Au

In this study, we fabricated an MMP2-recognizing UCNP. The nanoparticles were bound to gold nanoparticles, and did not emit fluorescence in response to 980-nm irradiation. The nanoparticles fluoresced by secreting MMP2 (Scheme 1).

NaYF4:Yb^{3+}/Er^{3+} nanoparticle (UCNP) was decorated with amino groups on a SiO_2 coated layer using 3-aminopropyl-triethoxysilane. The UCNP was coupled with peptides and folic acid using the NHS/EDC method, forming UCNP@p. The N-terminus of the peptide linkage included cysteine and protruded from peptide linkage of the UCNP@p. Thereafter, 3.5 nm gold nanoparticles were conjugated to the thiol group of cysteine to form an Au-S bound (Fig. 1A). The NaYF4:Yb^{3+}/Er^{3+} nanoparticle was a uniform sphere approximately 20 nm in size and stable (Fig. 1B). The UCNP@p was 40 nm in size, large than the UCNP, and exhibited a colloidal shape due to the SiO_2 coating. A 3-nm-thick silica shell was prepared by controlling the amount of tetraethyl orthosilicate (Fig. 1C). The gold nanoparticles ubiquitously surrounded the UCNP@p to form UCNP@p-Au (Fig. 1D).

The MMP-2 recognizing peptide was designed to consist of three parts from the N-terminus to the C-terminus. The amino acid sequence is CSGAVRWLLTA. The MMP2-recognizing cleavage site lies between tryptophan (W) and leucine (L). According to previous measurement, SGAVRWLLTA has a high kcat/Km ratio in MMP2 digestion compared with other MMPs (Chen et al. 2002). A cysteine residue was added to the head of SGAVRWLLTA, and this cysteine formed a bound with gold. (Dykman and Khlebtsov 2012; Kumar et al. 2013). The N-terminal amino acid

was acetylated to avoid a redundant reaction during the NHS/EDC coupling process. The carboxyl group of the peptide was able to couple with a decorated amino group on the silica coating on UCNP.

3.2. Optical property of UCNP@p-Au

NaYF4:Yb^{3+}/Er^{3+} was used as a core and surrounded by gold nanoparticles. In the upconversion fluorescence process, ytterbium acted as a sensitizer that was promoted to an excited state using 980-nm irradiation, during which electrons from the $^2F_{7/2}$ ground state jumped to the $^2F_{5/2}$ excited state(Chen and Zhao 2012). The unstable energy was then transferred to the unexcited erbium. The excited state of trivalent erbium released energy to emit fluorescence, including $^4F_{9/2} \rightarrow {}^4I_{15/2}$, $^4S_{3/2} \rightarrow {}^4I_{15/2}$, $^2H_{11/2} \rightarrow {}^4I_{15/2}$, and $^2H_{9/2} \rightarrow {}^4I_{15/2}$ transitions, which corresponded to wavelength of 400 nm, 520 nm, 540 nm and 650 nm, respectively (Fig. 2A).

Because gold is a noble metal, it can remove hydrogen atoms from the sulfur in cysteine to form an Au-S bond. The 3.5 nm gold nanoparticles served as a quenching moiety. The absorption of gold nanoparticles showed broad range in the visible spectrum and was especially pronounced at 530 nm (Fig. 2B). This optical absorption was able to quench the fluorescent emission from UCNP.

We first prepared UCNPs decorated with 2 mg of peptide using 1 mg of folic acid. The emission spectrum of the peptide-modified UCNP was effectively quenched by adding 0.24 μM of gold nanoparticles. Adding different concentrations of gold nanoparticle, the fluorescent emission of UCNP@p was significant inhibited using 980-nm irradiation (Fig. 2C). Increasing the gold nanoparticle concentration effectively quenched the strongest 540-nm emission (Fig. 2D).

3.3. In vitro MMP2 sensing analysis

Human recombinant MMP2 (rhMMP2) was used for the *in vitro* digestion of UCNP@p-Au. The MMP2 digestion was followed over time by adding 4 pg/ml rhMMP2 to 0.2 mg/ml of UCNP@p-Au and incubating the mixture at 37°C. The fluorescence intensity gradually increased over time (Fig. 3A). Although the upconversion fluorescence consisted of a composite emission, the dominant light was emitted at 540 nm. To delineate the rhMMP2 cleavage, we focused on the fluorescent

changes at 540 nm from UCNP@p. The exponential emission of MMP2-digested UCNP@p-Au is shown 20 minutes and 60 minutes. This enzyme reaction reached a plateau after 60 minutes (Fig. 3B).

The intensity of the upconversion fluorescence of UCNP@p-Au, a peak at 540 nm, positively correlated with the concentration of MMP2 from $4x10^{-4}$ to 40 pg/ml (Fig. 3C) and exhibited a linear relationship (Fig. 3D), indicating that the fluorescence intensity could be increased by increasing the amount of MMP2. We suggested that the limit of UCNP@p-Au was $4x10^{-4}$ pg/ml for *in vitro* MMP2-sensing. The fluorescence recovery indicated that the peptide linkage could be effectively digested by MMP2.

3.4. Cell sensing analysis of UCNP@p-Au for head and neck cancer cells

The UCNP@p-Au particles were used to sense in head and neck cancer cells. Considering the specific MMP2-recognizing peptide and folic acid decorations on the UCNP@p-Au, we assessed MMP2 and folate receptor expression in head and neck cancer cell lines (Fig. 4A). The folate receptor binds to folic acid on the surface of the UCNP@p and allows the cells to uptake nanoparticles. Several types of folate receptors exhibit a high affinity for folic acid (Paulmurugan et al. 2015; Zhao et al. 2015). MMP2 was significantly expressed in the FADU, HSC3, HSC4 and SAS cell lines. The folate receptor family, including folate receptor 1, folate receptor 2 and folate receptor 3, were further examined in the panel of cancer cell lines. Folate receptor 2 was ubiquitously expressed in head and neck cancer cell lines, despite the lower expression observed in HSC4, Ca922 and SAS cells. FADU and Cal27 cells were used in the cell sensing experiment with UCNP@p-Au. Specifically, 10 μg/ml of UCNP@p-Au was incubated with FADU and Cal27 cells for 12 hours. A nuclear fluorescent probe (DAPI) and an α-tubulin antibody were used to profile the localization of UCNP@p after MMP2 digestion and cell uptake. Cell sensing was assessed with a by fluorescent microscope using 980-nm irradiation. The fluorescent emission from UCNP was marked shown in FADU cells but not in Cal27 cells (Fig. 4B). As expected, FADU cells expressed higher levels of MMP2 than Cal27 cells, allowing them to be specifically sensed by UCNP@p-Au. Although the expression of folate receptors was equally expressed in FADU and Cal27 cells, Cal27 cells did not

emit fluorescence. Therefore, we hypothesize that MMP2 digestion did not occur in Cal27 cells. Furthermore, we proposed that UCNP@p-Au can be used as a biosensor for head and neck cancer cells, which express MMP2.

3.5. Safety analysis of UCNP@p-Au

The cytotoxicity of the head and neck cancer cell lines, FADU and Cal27, was determined using an Alamar blue assay. MMP2 overexpression is usually involved in local cancer cell invasion and distant metastasis, leading to a poor prognosis in head and neck cancer(Lotfi et al. 2015). Most head and neck cancers can be effectively cured by surgery in the early stages. However, the head and neck cancer commonly undergoes highly lymph node metastasis and lack a suitable marker for early diagnosis (Xing et al. 2015). Thus, we selected MMP2 as a diagnostic factor for head and neck cancer. To determine the cytotoxicity of the UCNP@p-Au system, different concentrations of sensor nanoparticles were incubated with head and neck cancer cells. After 48 hours of incubation, the UCNP@p-Au particles exhibited slight cytotoxicity in FADU and Cal27 cancer cells (Fig. 5A). Nevertheless, over 95% of cells survived when the concentration of UCNP@p-Au was increased. Moreover, the cells were cultured with UCNP@p-Au for up to seven days (Fig. 5B). The 250 μg/ml concentration was slightly cytotoxic in long term incubation. This result indicated that the 83μg/ml dose is the maximal dosage for cancer cell sensing. Overall, the UCNP@p-Au particles were minimally cytotoxicity and biocompatible.

3.6. Visualization of cell sensing in MMP2 overexpressing cell line

We overexpressed MMP2 in a cell line using a lentivirus. Specifically, Cal27 cells, which express low levels of MMP2, were infected with an MMP2-overexpressing virus; control cells were infected with a vector control. The stably transduced cell lines were named Cal27/MMP2 and Cal27/VC, respectively. The Cal27/MMP2 cells express significantly more MMP2 than the Cal27/VC cells (Fig. 6A). Because MMP2 is a bio-active secreted protein, we collected the conditioned medium (serum-free) from cell culture, concentrated it 50-fold and dissolved it in PBS. Cal27/MMP2 secreted MMP2 (Fig. 6A, bottom). A 10 μg aliquot of conditioned mediums containing the total proteins secreted by Cal27/VC and Cal27/MMP2 cells was

subjected to MMP2-sensing using 0.2 mg/ml UCNP@p-Au solution (Fig. 6B). As described by the emission spectrum, upconversion fluorescence significantly increase when mixing the UCNP@p-Au and medium from Cal27/MMP2. Hence, MMP2 was active and secreted from Cal27/MMP2 but not Cal27/VC. Corresponding to a previous report, MMP2 was actively being secreted from the cell(Theret et al. 1999). Subsequently, UCNP@p-Au was applied to Cal27/MMP2 cells. Significant fluorescence was significantly observed in the Cal27/MMP2 cell line (Fig. 6C), indicating that the UCNP@p-Au is an effective sensor.

4. Conclusion

MMP2 specific peptides have been extensively developed as a MMP2 sensor. In this study, we successfully fabricated an MMP2-sensing upconversion nanoparticle. This particle, termed UCNP@p-Au consisted primarily of folic acid, a MMP2-recognizing peptide, AuNP and UCNP. The UCNPs emitted green fluorescence in response to 980-nm irradiation but exhibited quenching because of AuNPs that were close to the UCNPs. An MMP2-specific peptide conjugated to UCNP and AuNP, was cleaved by MMP2 protein *in vivo* and *in vitro*. Moreover, UCNP@p-Au exhibited low cytotoxicity and may employed to sense MMP2 secreted by head and neck cancer cells. Furthermore, UCNP@p-Au may serve as a clinical diagnostic tool for monitoring the malignant cancer cells via dynamic imaging.

Acknowledgements

We thank the Academia Sinica (Contract No.AS-103-TP-A06) for financially supporting this work. We also thank the GRC Peptide Synthesis Core Facilities for supporting the peptide synthesis. The authors would like thank the Ministry of Science and Technology of Taiwan (Contract Nos. MOST 104-2745-M-002-003-ASP and MOST 104-2113-M-002-012-MY3).

Author Contributions Statement

Yung-Chieh Chan and Michael Hsiao designed and performed the experiments, and co-wrote the manuscript. Chieh-Wei Chen, Ming-Hsien Chan, Yu-Chang Chang, Wei-Min Chang, Li-Hsing Chi, Hui-Ming Yu and Yuan-Feng Lin provided technical support and materials. Din Ping Tsai and Ru-Shi Liu discussed the data, and developed the theoretical aspect and wrote the manuscript. All authors commented on the manuscript.

Additional Information

Competing Financial Interests Statement

The authors declare no competing financial interests.

Scheme 1.

Illustration of the UCNP@p-Au sensed by MMP2-expressing cancer cells. UCNP@p-Au was colorless under 980-nm irradiation, and MMP2-digested UCNP was taken by the cell, as detected using 980-nm irradiation.

Figure legends

1. (A) Schematic showing the process of UCNP@p-Au fabrication. TEM image of (B) the UCNP (C) the peptide-modified UCNP (D) 3.5 nm gold NP conjugated with peptide-modified UCNP. The scale bar indicated to 50 nm.
2. (A) Fluorescence spectra of upconversion nanoparticle. (B) The absorption of 3.5 nm gold nanoparticle. (C) Upconversion spectra of the peptide-modified UCNP conjugated with various concentration of 3.5 nm gold nanoparticle. (D) Upconversion spectra of folic acid and peptide-modified UCNP with various concentrations of gold
3. Time-dependent and dose-dependent fluorescence intensity of UCNP@p-Au in the presence of MMP2 recombinant protein. (A) The digestion of MMP2 is shown as a function of time using the photoluminescence spectrum; specifically, 0.2 mg/ml of UCNP@p-Au solution was incubated with 4 pg/ml of human recombinant MMP2 protein. The emission was measured at 0, 15, 30, 45, 60 and 120 minutes. (B) The maximum emission at 540 nm increased as a function of time. (C) UCNP@p-Au can sense different doses of rhMMP2 from $4x10^{-4}$ to 40 (pg/ml), which constitutes a 10-fold difference in concentration. (D) A trend line indicated that UCNP@p-Au was able to sense to different concentrations of rhMMP2. The X-axis represents the treatment dosage (pg/ml). Data from three independent experiments are presented as the means± SEs
4. (A) Western blot for determining the protein levels of endogenous MMP2 and folic acid receptor (FOLR). (B) Cal27 and FADU were treated with UCNP@p-Au for 12 hours. The cells were immunofluorescently stained, and observed by fluorescence microscopy under 980-nm irradiation.
5. Cell viability assay showing the head and neck cancer cell lines of FADU and Cal27 incubated with UCNP@p-Au (A) for 24 hours (B) for a long-term incubation.

6. MMP2 was expressed in the MMP2-deficient cell line, Cal27. (A) The western blot demonstrated that MMP2 was overexpressed in Cal27/MMP2 but not the control vector-infected cell, Cal27/VC. β-actin served as internal control for cell lysates. The extracellular MMP2 expression (medium) is shown at the bottom. (B) Extracellular MMP2s were detected by upconversion fluorescence in the UCNP@p-Au solution. (C) Cell sensing was evident for Cal27/MMP2 and Cal27/VC cells.

Scheme1

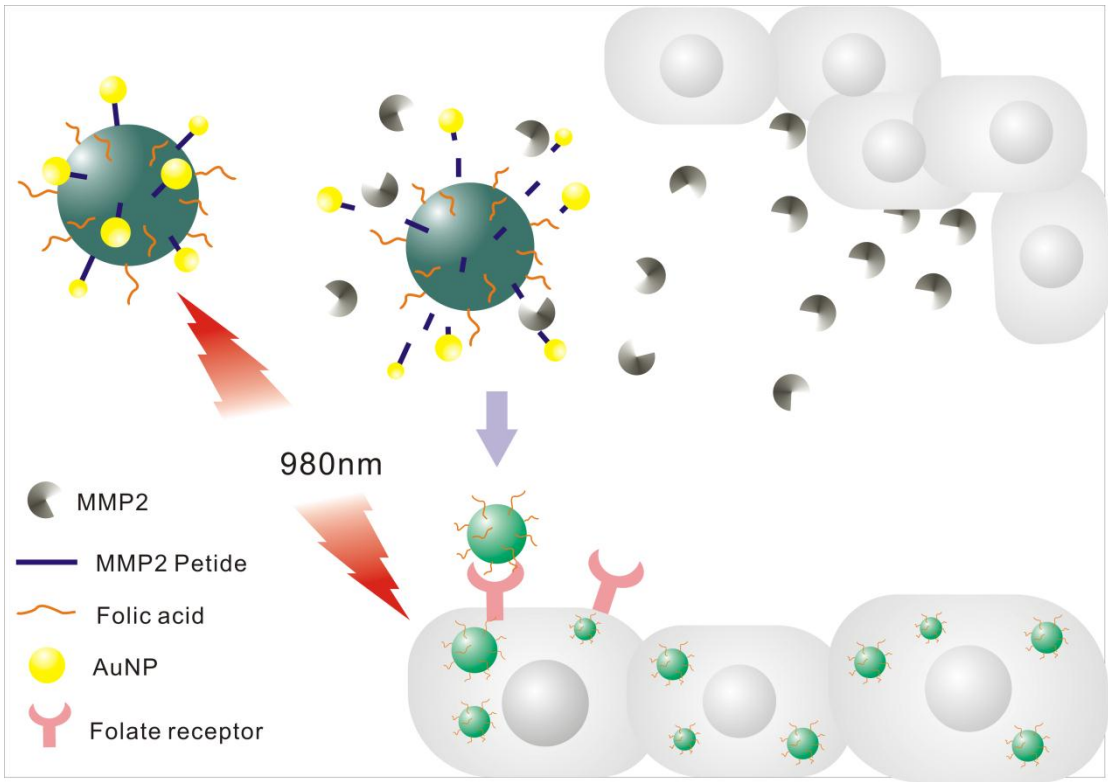

Figure 1

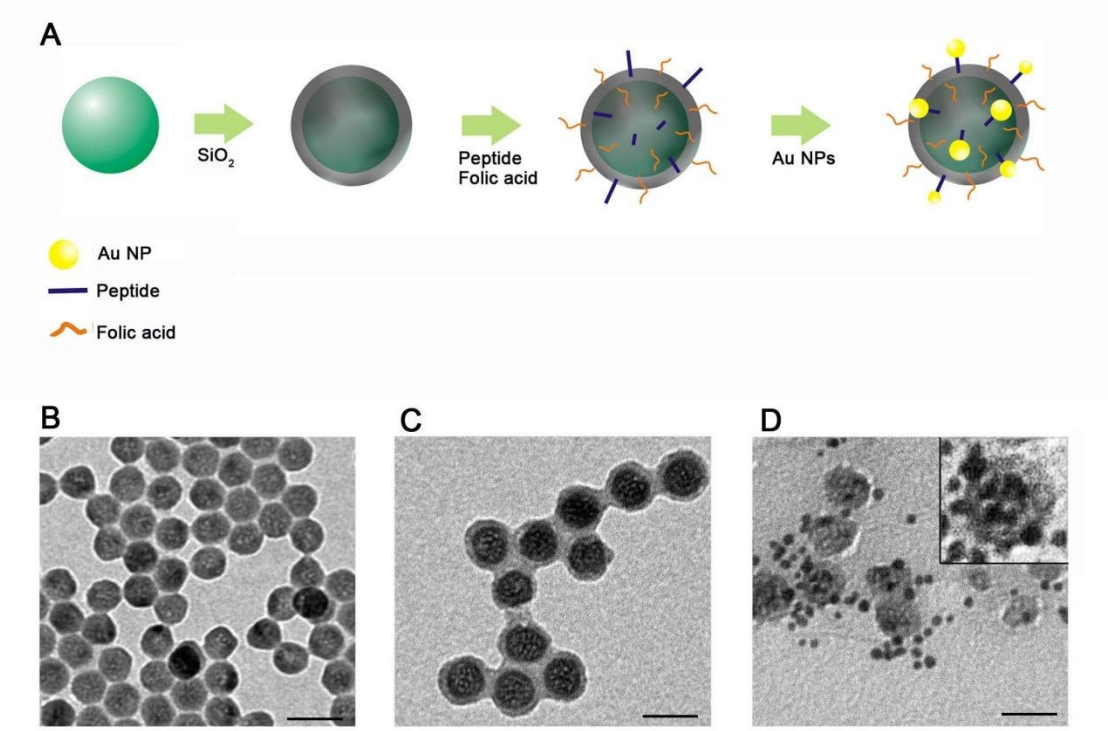

Figure 2

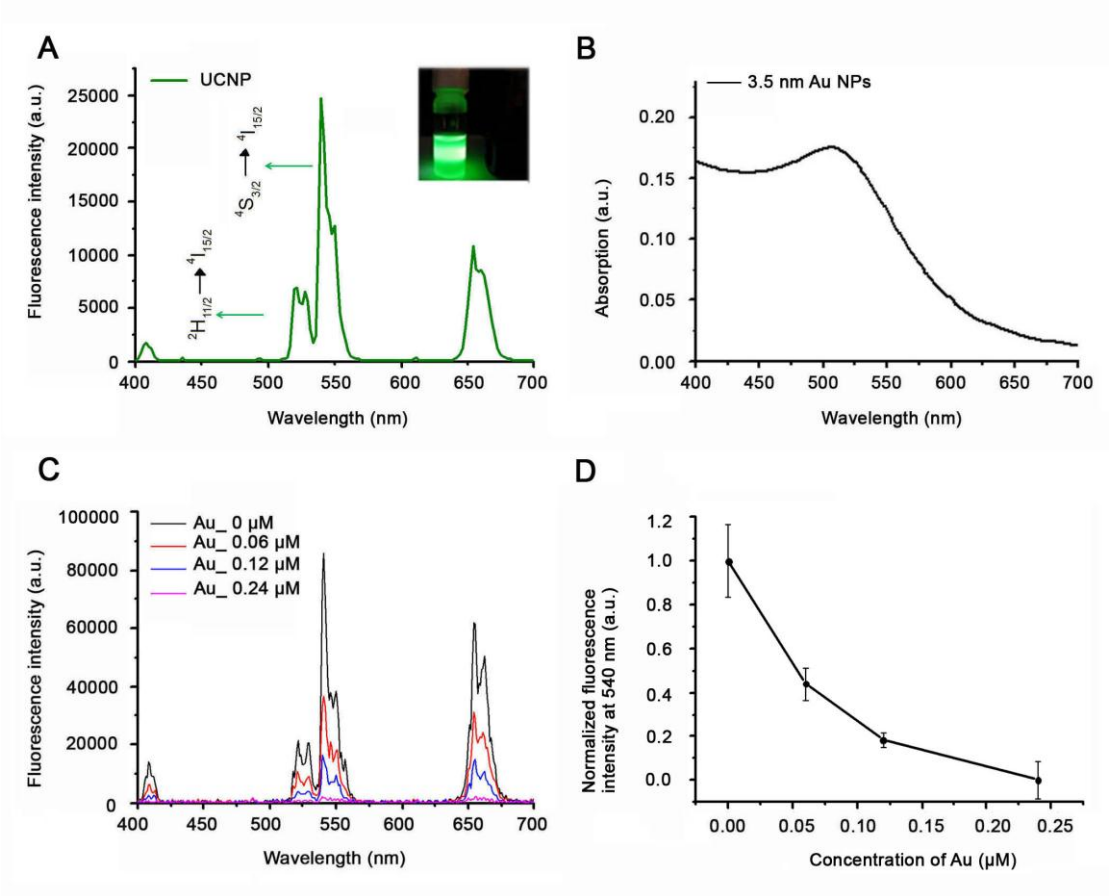

Figure 3

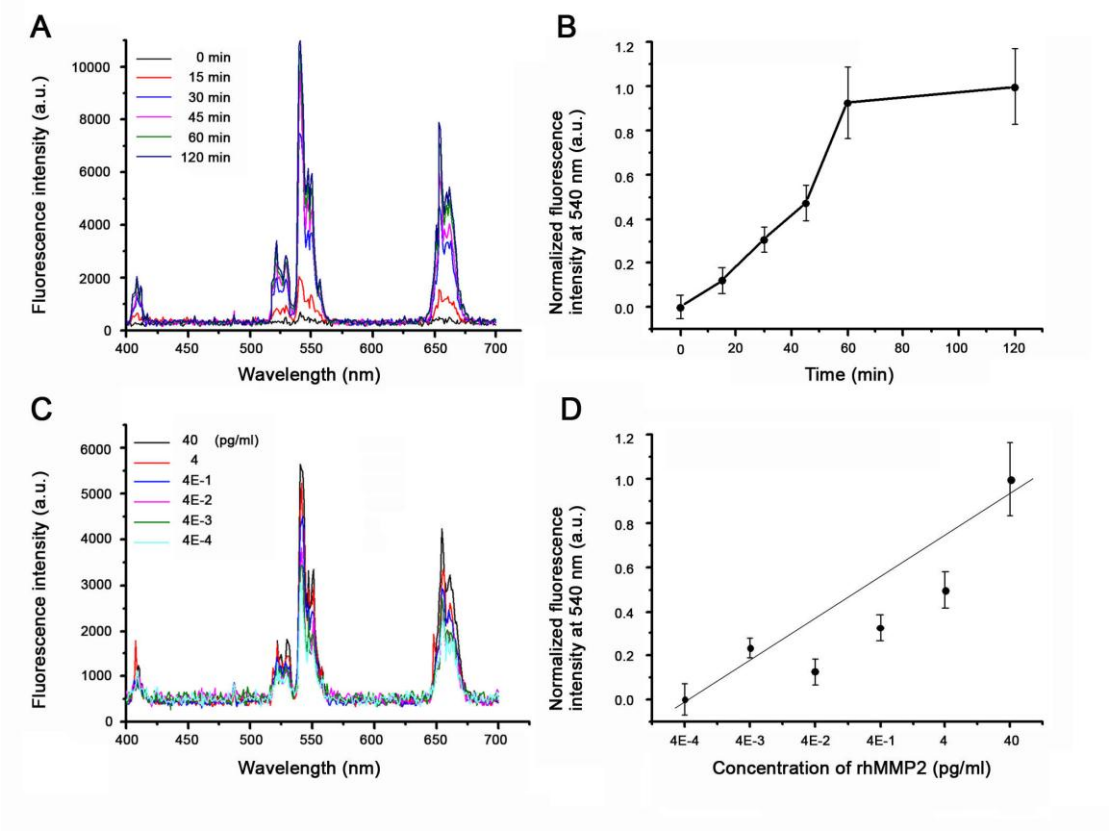

Figure 4

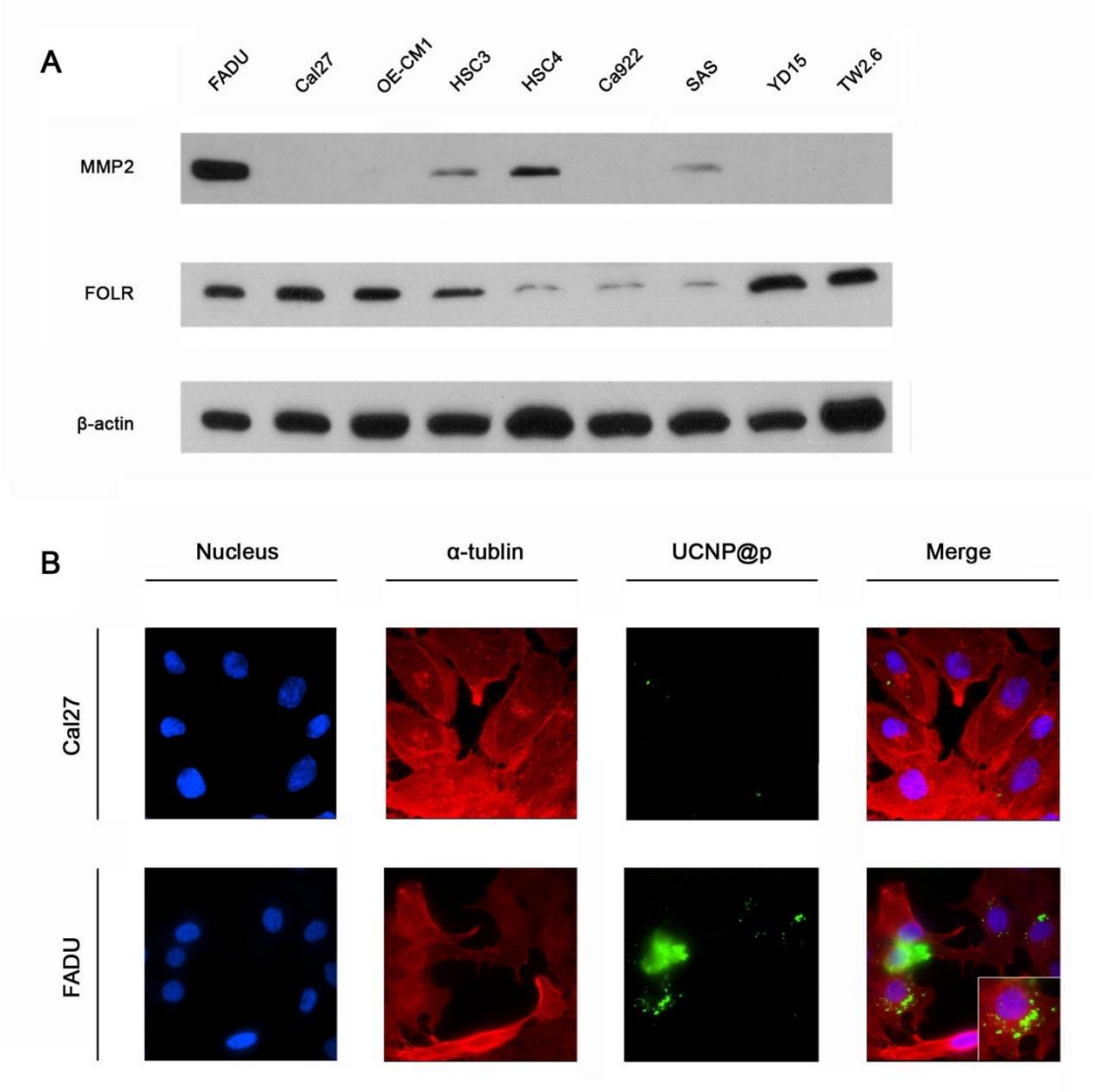

Figure 5

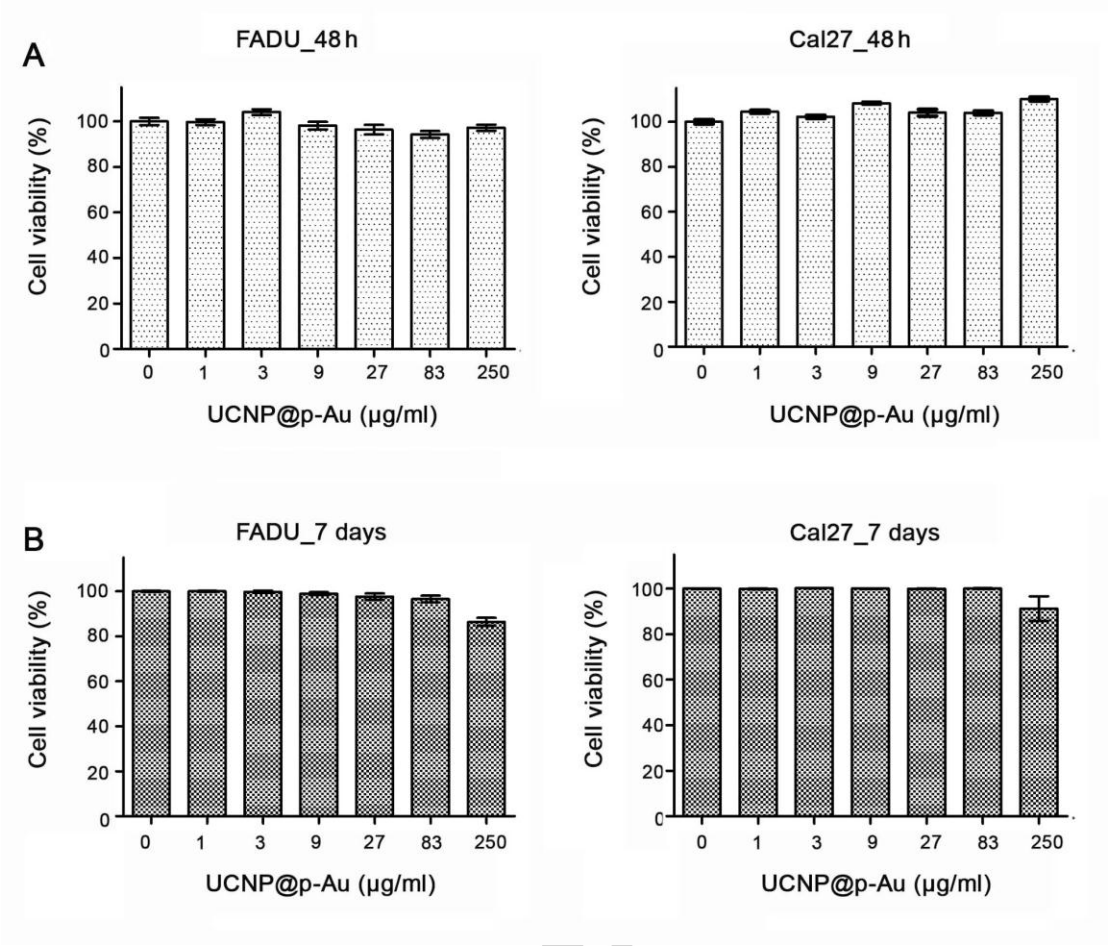

Figure 6

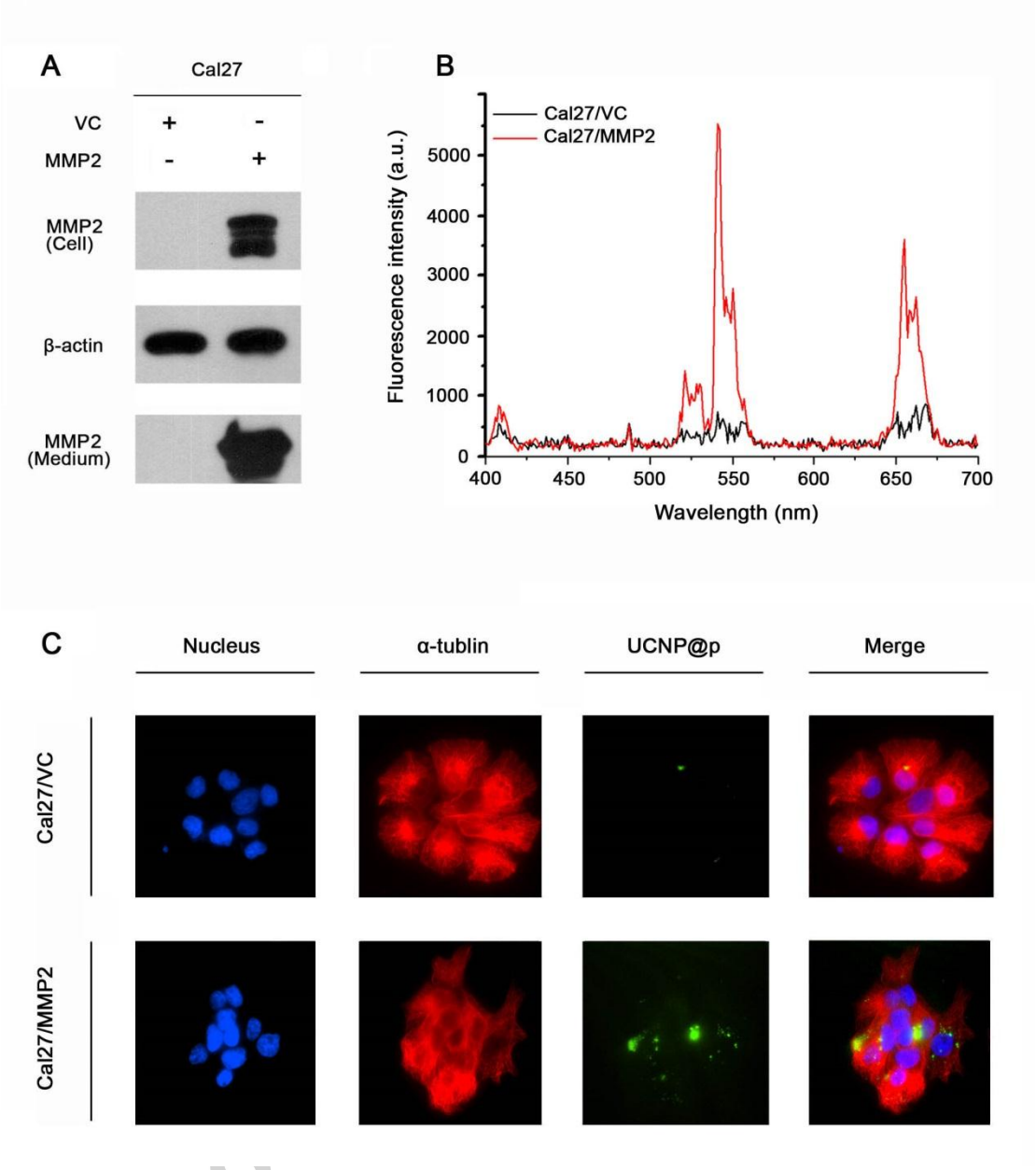

Reference

Adabi, Z., Mohsen Ziaei, S.A., Imani, M., Samzadeh, M., Narouie, B., Jamaldini, S.H., Afshari, M., Safavi, M., Roshandel, M.R., Hasanzad, M., 2015. Genetic Polymorphism of MMP2 Gene and Susceptibility to Prostate Cancer. Archives of medical research 46(7), 546-550.

Banerjee, K., Resat, H., 2015. Constitutive activation of STAT3 in breast cancer cells: A review. International journal of cancer. Journal international du cancer.

Chen, C.-W., Lee, P.-H., Chan, Y.-C., Hsiao, M., Chen, C.-H., Wu, P.C., Wu, P.R., Tsai, D.P., Tu, D., Chen, X., Liu, R.-S., 2015. Plasmon-induced hyperthermia: hybrid upconversion NaYF4:Yb/Er and gold nanomaterials for oral cancer photothermal therapy. Journal of Materials Chemistry B 3(42), 8293-8302.

Chen, E.I., Kridel, S.J., Howard, E.W., Li, W., Godzik, A., Smith, J.W., 2002. A unique substrate recognition profile for matrix metalloproteinase-2. The Journal of biological chemistry 277(6), 4485-4491.

Chen, J., Zhao, J.X., 2012. Upconversion nanomaterials: synthesis, mechanism, and applications in sensing. Sensors (Basel, Switzerland) 12(3), 2414-2435.

Dykman, L., Khlebtsov, N., 2012. Gold nanoparticles in biomedical applications: recent advances and perspectives. Chemical Society reviews 41(6), 2256-2282.

Eftekhary, H., Ziaee, A.A., Yazdanbod, M., Shahpanah, M., Setayeshgar, A., Nassiri, M., 2015. The influence of matrix metalloproteinase-2, -9, and -12 promoter polymorphisms on Iranian patients with oesophageal squamous cell carcinoma. Contemporary oncology (Poznan, Poland) 19(4), 300-305.

Frankowski, H., Gu, Y.-H., Heo, J.H., Milner, R., del Zoppo, G.J., 2012. Use of Gel Zymography to Examine Matrix Metalloproteinase (Gelatinase) Expression in Brain Tissue or in Primary Glial Cultures. Methods in molecular biology (Clifton, N.J.) 814, 221-233.

Gong, T., Kong, K.V., Goh, D., Olivo, M., Yong, K.T., 2015. Sensitive surface enhanced Raman scattering multiplexed detection of matrix metalloproteinase 2 and 7 cancer markers. Biomedical optics express 6(6), 2076-2087.

Gong, Y., Chippada-Venkata, U.D., Oh, W.K., 2014. Roles of matrix metalloproteinases and their natural inhibitors in prostate cancer progression. Cancers 6(3), 1298-1327.

Holle, A.W., Young, J.L., Spatz, J.P., 2015. In vitro cancer cell-ECM interactions

inform in vivo cancer treatment. Advanced drug delivery reviews.
Jafarian, A.H., Vazife Mostaan, L., Mohammadian Roshan, N., Khazaeni, K., Parsazad, S., Gilan, H., 2015. Relationship between the Expression of Matrix Metalloproteinase and Clinicopathologic Features in Oral Squamous Cell Carcinoma. Iranian journal of otorhinolaryngology 27(80), 219-223.
Kumar, A., Zhang, X., Liang, X.J., 2013. Gold nanoparticles: emerging paradigm for targeted drug delivery system. Biotechnology advances 31(5), 593-606.
Kwan, J.A., Schulze, C.J., Wang, W., Leon, H., Sariahmetoglu, M., Sung, M., Sawicka, J., Sims, D.E., Sawicki, G., Schulz, R., 2004. Matrix metalloproteinase-2 (MMP-2) is present in the nucleus of cardiac myocytes and is capable of cleaving poly (ADP-ribose) polymerase (PARP) in vitro. FASEB journal : official publication of the Federation of American Societies for Experimental Biology 18(6), 690-692.
Li, S.Y., Liu, L.H., Cheng, H., Li, B., Qiu, W.X., Zhang, X.Z., 2015. A dual-FRET-based fluorescence probe for the sequential detection of MMP-2 and caspase-3. Chemical communications (Cambridge, England) 51(77), 14520-14523.
Li, Z., Wang, L., Wang, Z., Liu, X., Xiong, Y., 2011. Modification of NaYF4:Yb,Er@SiO2 Nanoparticles with Gold Nanocrystals for Tunable Green-to-Red Upconversion Emissions. The Journal of Physical Chemistry C 115(8), 3291-3296.
Liu, Q., Pan, D., Cheng, C., Zhang, D., Zhang, A., Wang, L., Jiang, H., Wang, T., Liu, H., Xu, Y., Yang, R., Chen, F., Yang, M., Zuo, C., 2015a. Development of a Novel PET Tracer [18F]AlF-NOTA-C6 Targeting MMP2 for Tumor Imaging. PloS one 10(11), e0141668.
Liu, Y.P., Lee, J.J., Lai, T.C., Lee, C.H., Hsiao, Y.W., Chen, P.S., Liu, W.T., Hong, C.Y., Lin, S.K., Ping Kuo, M.Y., Lu, P.J., Hsiao, M., 2015b. Suppressive function of low-dose deguelin on the invasion of oral cancer cells by downregulating tumor necrosis factor alpha-induced nuclear factor-kappa B signaling. Head & neck.
Lotfi, A., Mohammadi, G., Tavassoli, A., Mousaviagdas, M., Chavoshi, H., Saniee, L., 2015. Serum levels of MMP9 and MMP2 in patients with oral squamous cell carcinoma. Asian Pacific journal of cancer prevention : APJCP 16(4), 1327-1330.
Paulmurugan, R., Bhethanabotla, R., Mishra, K., Devulapally, R., Foygel, K., Sekar, T.V., Ananta, J.S., Massoud, T.F., Joy, A., 2015. Folate Receptor Targeted Polymeric Micellar Nanocarriers for Delivery of Orlistat as a Repurposed Drug against Triple Negative Breast Cancer. Molecular cancer therapeutics.

Shao, B., Yang, Z., Wang, Y., Li, J., Yang, J., Qiu, J., Song, Z., 2015. Coupling of Ag Nanoparticle with Inverse Opal Photonic Crystals as a Novel Strategy for Upconversion Emission Enhancement of NaYF: Yb, Er Nanoparticles. ACS applied materials & interfaces.

Theocharis, A.D., Skandalis, S.S., Gialeli, C., Karamanos, N.K., 2015. Extracellular Matrix Structure. Advanced drug delivery reviews.

Theret, N., Lehti, K., Musso, O., Clement, B., 1999. MMP2 activation by collagen I and concanavalin A in cultured human hepatic stellate cells. Hepatology (Baltimore, Md.) 30(2), 462-468.

Xing, Y., Zhang, J., Lin, H., Gold, K.A., Sturgis, E.M., Garden, A.S., Lee, J.J., William, W.N., Jr., 2015. Relation between the level of lymph node metastasis and survival in locally advanced head and neck squamous cell carcinoma. Cancer.

Xu, H., Li, M., Zhou, Y., Wang, F., Li, X., Wang, L., Fan, Q., 2015. S100A4 participates in epithelial-mesenchymal transition in breast cancer via targeting MMP2. Tumour biology : the journal of the International Society for Oncodevelopmental Biology and Medicine.

Yang, J.R., Pan, T.J., Yang, H., Wang, T., Liu, W., Liu, B., Qian, W.H., 2015. Kindlin-2 promotes invasiveness of prostate cancer cells via NF-kappaB-dependent upregulation of matrix metalloproteinases. Gene.

Zhang, F., Wang, Z., Fan, Y., Xu, Q., Ji, W., Tian, R., Niu, R., 2015. Elevated STAT3 Signaling-Mediated Upregulation of MMP-2/9 Confers Enhanced Invasion Ability in Multidrug-Resistant Breast Cancer Cells. International journal of molecular sciences 16(10), 24772-24790.

Zhao, R., Visentin, M., Goldman, I.D., 2015. Determinants of the activities of antifolates delivered into cells by folate-receptor-mediated endocytosis. Cancer chemotherapy and pharmacology 75(6), 1163-1173.

Zhong, Y., Rostami, I., Wang, Z., Dai, H., Hu, Z., 2015. Energy Migration Engineering of Bright Rare-Earth Upconversion Nanoparticles for Excitation by Light-Emitting Diodes. Advanced materials (Deerfield Beach, Fla.).

Zou, M., Zhang, X., Xu, C., 2015. IL6-induced metastasis modulators p-STAT3, MMP-2 and MMP-9 are targets of 3,3'-diindolylmethane in ovarian cancer cells. Cellular oncology (Dordrecht).

Highlights

1. We fabricated an MMP2-recognizing upconversion nanoparticle that emitted fluorescence in response to active MMP2 secreted from head and neck cancer cells.
2. UCNPs were coated a silica shell and further conjugated with MMP-recognizing polypeptides and folic acid.
3. We used 3.5-nm gold nanoparticles as a quencher that absorbed the upconversion fluorescence from UCNP.
4. MMP2-recognizing upconversion nanoparticles can be endocytosed by head and neck cancer cells, are biocompatible with little toxicity.